

POLAR ORBITER WIND AND HEIGHT ESTIMATION

G.G. Campbell

Center for Geosciences/Atmospheric Research
Colorado State University

Ft. Collins, CO. 80302 USA

970 491 8497
campbell@cira.colostate.edu

ABSTRACT

Estimating cloud motions and heights in polar regions away from areas observed by geosynchronous satellites is a particularly important problem for military operations. Using POLDER 6 km resolution pixels shows height and motion can be derived, but just above the noise level. High resolution observations would provide useful results.

OBJECTIVE

Measurement of geometric cloud height and motion measurements have been demonstrated with GOES (Campbell, 1998) data and Meteosat data (Campbell and Holmlund, 2000). The objective of this study is to apply the same techniques to polar orbiter data, especially in polar areas because those are not observed by geosynchronous satellites. With several polar orbiter imager observations from different satellites like DMSP, Defense Meteorological Satellite Program, Operational Linescan System, and NOAA AVHRR, Advanced Very High Resolution Radiometer, one can see displacements of clouds in the images due to parallax and motion since the images are not likely to be simultaneous and have different view points. The basic question is: "Can the parallax and motion be separated to estimate velocity and height?". This is not possible with single view instruments, but multiple-view instruments offer a unique opportunity.

The POLDER, Polarization and Directionality of the Earth's Reflectances, instrument contains several array detectors which view the earth as that satellite moves in its orbit. This allows the observation of the surface below up to 14 times at different view angles within 4 minutes (Deschamps et al 1994). It was originally designed for bi-directional reflectance measurements, but this is a test of stereo heights estimates. The sequence of POLDER views were mapped into a common projection assuming the reflecting object came from the surface of the earth. Any displacement from one view to an other is due to the fact that the cloud is above the surface (parallax) or has moved (wind) between the measurement times. A similar but higher resolution system, MISR, Multi-Angle Imaging Spectro-Radiometer, is now flying on the Terra space craft.

Simulations

To examine the measurement problem, we first simulated the observation system. There is a fundamental uncertainty in tracking clouds because one must align the edge of the cloud from one image to the next. Let us represent the apparent location of the cloud as \mathbf{P} which is the projection of the cloud location, \mathbf{R}_c , to the mapping surface (Earth's geoid) from the satellite view point, \mathbf{S} . This includes the alignment errors and the round off errors due to the resolution of the image. In addition the cloud can move in time with velocity \mathbf{V} , as the multiple observations are made. Finally several view points from one satellite or many satellites could be used to observe the cloud. (Notice that \mathbf{P} , \mathbf{R} , \mathbf{S} and \mathbf{V} are vectors.)

$$\mathbf{P}_i(t) = \mathbf{R}_c(t) + \gamma(\mathbf{S}_i - \mathbf{R}_c(t)) \quad 1.$$

Equation 1 says that the apparent location of a cloud edge, \mathbf{P} , is the true location plus some fraction, γ , of the vector connecting the view point, \mathbf{S} , and the cloud edge, \mathbf{R}_c . Then replacing the cloud location with as starting point and the motion vector times the time we get equation 2.

$$\mathbf{P}_i(t) = \mathbf{R}_c(0) + \mathbf{V}t + \gamma(\mathbf{S}_i - \mathbf{R}_c(0) - \mathbf{V}t) \quad 2.$$

With a set of observations, $\mathbf{P}_i(t)$, one can solve for $\mathbf{R}_c(0)$ and \mathbf{V} with a least squares fit. This method has been described by Campbell (1998) as the asynchronous stereo height and motion analysis system. The projection constant, γ , also falls out of the solution. Unfortunately, for some special cases, there is a redundancy between $\mathbf{R}_c(0)$ and \mathbf{V} for certain sequences of observation locations \mathbf{S}_i in a plane. Physically as the satellite moves in its orbit the sequence of $\mathbf{P}_i(t)$ can be produced by different parallax values for a high cloud or by the movement of the cloud parallel to the orbit track at a different height. This occurs from one satellite like POLDER. Adding an additional satellite view point off the POLDER orbit plane, allows a unique solution. The short interval of the observations from sun synchronous orbits, less than 300 seconds, also limits the accuracy because the cloud can not move very far in the interval. So, an observation at 1000 seconds or more away in time is more effective ie from a AVHRR or DMSP imager.

To estimate the error of this measurement system we used a boot strap statistical method. Many sequences of measurements from one orbit with added random locations errors were analyzed, and the standard deviation of the solutions give an estimate of the uncertainty. Five cases were considered: including 11 observations from a satellite at 800 km altitude at 20 second intervals and the addition of one extra satellite observation.

Case 1 had $\mathbf{V}=0$. plus an other measurement off to the side 1000 seconds later from 900km altitude like an AVHRR observation off to the side, not on the POLDER orbit plane.

Case 2 had motion =10m/sec in the cross track (U) direction plus AVHRR.

Case 3 had motion =10m/sec in the along track (V) direction plus AVHRR.

Case 4 had motion =10m/sec in the cross track (U) direction plus an other measurement off to the side 1000 seconds later from 36000 km altitude (geosynchronous satellite).

Case 5 had motion =10m/sec in the along track (V) direction plus geosynchronous

| Error km | $\pm .3$ | $\pm 1.$ | $\pm 2.$ | $\pm 3.$ | $\pm .3$ | $\pm 1.$ | $\pm 2.$ | $\pm 3.$ |
|----------|---------------------------------|----------|----------|----------|---------------------------|----------|----------|----------|
| | Case 1 U=0,V=0, H = 10. | | | | | | | |
| H km | 0.05 | 0.47 | 2.00 | 4.37 | | | | |
| U m/sec | 0.34 | 4.30 | 15.70 | 36.79 | | | | |
| V m/sec | 0.09 | 1.05 | 3.94 | 9.46 | | | | |
| | Case 2 U=10,V=0 P + AVHRR | | | | Case 3 U=0,V=10 P + AVHRR | | | |
| H km | 0.05 | 0.55 | 2.02 | 4.51 | 0.05 | 0.52 | 2.07 | 4.49 |
| U m/sec | 0.26 | 2.93 | 12.67 | 26.37 | 0.26 | 2.85 | 11.38 | 24.54 |
| V m/sec | 0.09 | 1.11 | 4.19 | 8.72 | 0.10 | 1.10 | 4.32 | 10.52 |
| | Case 4 U=10 V=0, H=10, P + GOES | | | | Case 5 U=0,V=10 P + GOES | | | |
| H km | 0.04 | 0.51 | 2.13 | 4.70 | 0.05 | 0.53 | 2.26 | 5.13 |
| U m/sec | 0.12 | 1.46 | 5.26 | 11.75 | 0.10 | 1.08 | 3.80 | 8.91 |
| V m/sec | 0.10 | 1.04 | 4.47 | 9.38 | 0.12 | 1.19 | 4.91 | 12.01 |

Table 1: Standard errors for a multiple view instrument (11 views) with different random location errors. An additional satellite view was included 1000 seconds later.

Different error levels between ± 0.3 km and $\pm 3.$ km were added as shown in the table 1. At ± 3 km location error, the noise generally overwhelms the signal, so fairly precise locations are required for deriving useful results. The operational cloud tracking errors are around ± 8 m/sec and cloud heights at ± 1 km (Menzel, 2000). The results with 1 km locations errors would then be competitive with the operational algorithms. But those are applied to geosynchronous observations, and our goal here is an algorithm for polar areas. Empirically the tracking errors of the POLDER observations are around 2 km as seen in the examples shown below. For the MISR instrument on the NASA Terra satellite, location errors are probably better than ± 0.3 km which will provide excellent results if accurate matching AVHRR data can be obtained.

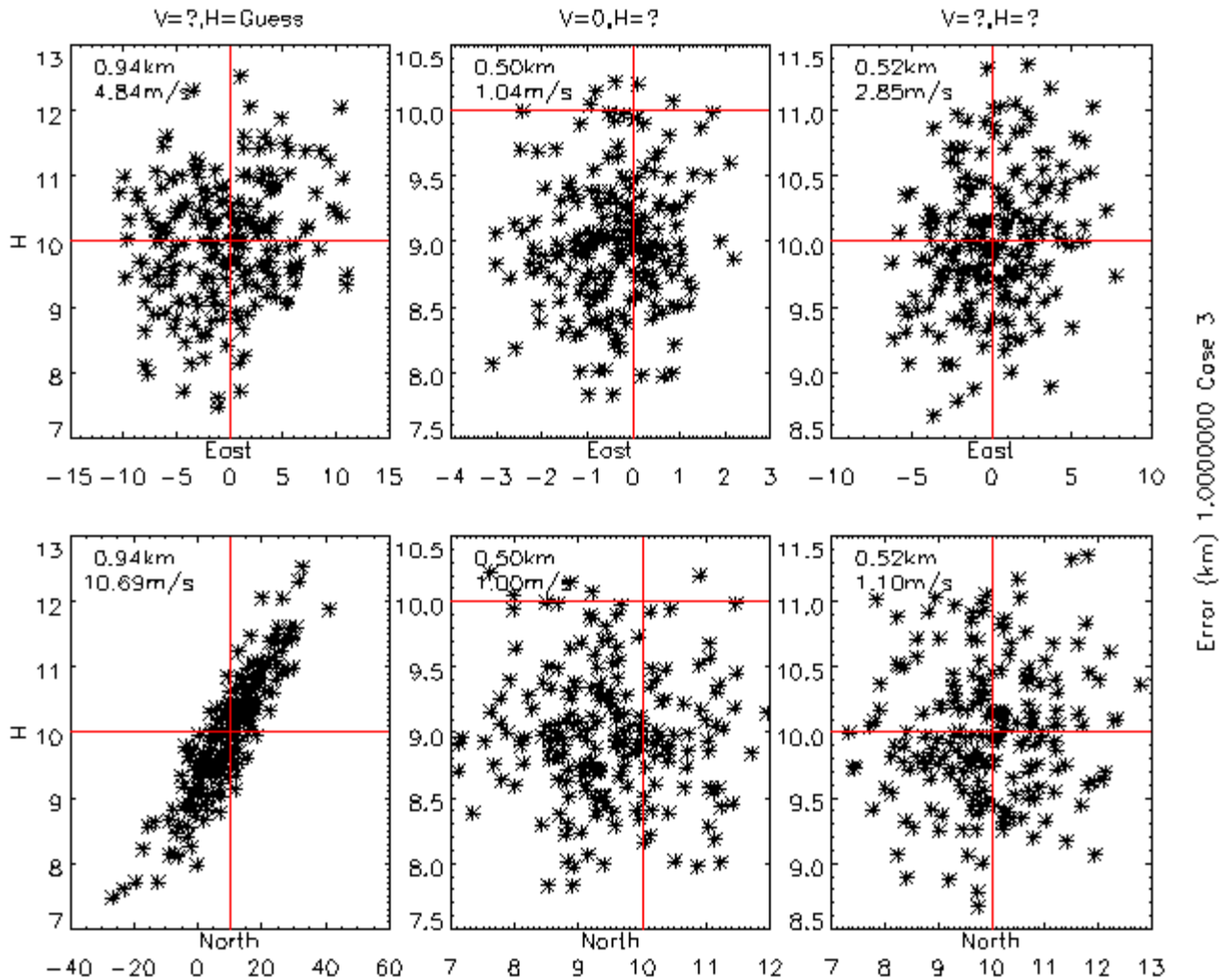


Figure 1 Each random simulated result showing the Height (H km) and the U (East m/sec) and V (North m/sec) components of the motion. These are simulations for error of ± 1 km for case 3 (POLDER + AVHRR). All the vertical axes show the heights. The cross hair in the middle of the plots show the correct solution. The right pair show that the full solution with two satellites has a symmetric distribution and random errors will not bias the results. The left pair are from the analysis using only one satellite and a imposed cloud height with uncertainty of ± 1 km. Systematic errors will arise from that case, with clouds assigned a high location moving one way and those assigned too low a height moving the opposite direction. The central pair are an analysis with the assumption of zero velocity to derive the height and then an analysis like the left pair for motion using that height. Here significant systematic errors appear in the estimate heights.

With different assumptions, two other analysis algorithms are possible. If separate information on cloud height could be obtained, then the multiple view satellite can be operated to just track the clouds in time. This has the problem that the clouds will not move very far in the short time interval of the fly over. Table 2 shows as simulation of that situation with random errors added to the input cloud height. Some of the redundancy between height and along track motion still seeps into the solution as seen in the along track, V, error even with the smallest location errors. This is also seen in the left portion of figure 1. The addition of an extra satellite improves the determination of the motion.

A third method would be to solve for the height assuming no motion (or saying the observed shifts are just due to parallax). Then repeat the analysis like the second algorithm with the height as input. Figure 1 shows the scatter of results with these three analysis schemes. The important result is that systematic biases will arise because height errors will be correlated with derived along track velocity errors for two approximate algorithms.

| Error km | $\pm .3$ | $\pm 1.$ | $\pm 2.$ | $\pm 3.$ | $\pm .3$ | $\pm 1.$ | $\pm 2.$ | $\pm 3.$ |
|----------|---------------------------|----------|----------|----------|---------------------------|----------|----------|----------|
| | Case 1 U=0,V=0, H = 10. | | | | | | | |
| H km | 0.26 | 0.94 | 2.06 | 2.82 | | | | |
| U m/sec | 0.40 | 4.93 | 18.19 | 44.54 | | | | |
| V m/sec | 2.57 | 10.44 | 27.06 | 49.47 | | | | |
| | Case 2 U=10,V=0 P + AVHRR | | | | Case 3 U=0,V=10 P + AVHRR | | | |
| H km | 0.27 | 1.09 | 1.99 | 3.24 | 0.30 | 0.94 | 2.03 | 2.95 |
| V m/sec | 0.40 | 4.54 | 19.09 | 45.14 | 0.42 | 4.84 | 18.10 | 39.15 |
| U m/sec | 2.67 | 12.22 | 28.04 | 52.13 | 2.99 | 10.69 | 27.02 | 51.21 |
| | Case 4 V=, H=10, P + GOES | | | | Case 5 U=0,V=10 P + GOES | | | |
| H km | 0.31 | 0.97 | 1.83 | 3.08 | 0.28 | 1.00 | 1.89 | 2.95 |
| U m/sec | 0.44 | 4.65 | 17.83 | 42.81 | 0.41 | 4.47 | 18.12 | 42.12 |
| V m/sec | 3.08 | 9.99 | 25.31 | 53.73 | 2.81 | 10.73 | 26.80 | 49.88 |

Table 2: Standard errors for a single multiple view instrument (11 views) with different random location errors using the assumed height algorithm. The error applied to the height as well as each location.

Finally there is another possible analysis scheme for two satellites flying in formation. This often happens when two DMSP satellites are in the same orbit as an older satellite is being replaced. In this case the viewpoint angles are nearly identical from the two views up to 30 minutes apart. Then the cloud motion is just the apparent displacement between the two successive images from the two satellites. Unfortunately there is no geometric information on the cloud height in this case, but a third satellite from a different orbit might be available to provide a solution. Formation flying of two satellites is not common for operational satellites, so the practicality of this algorithm is not high.

| Error km | $\pm .3$ | $\pm 1.$ | $\pm 2.$ | $\pm 3.$ | $\pm .3$ | $\pm 1.$ | $\pm 2.$ | $\pm 3.$ |
|----------|-------------------------|----------|----------|----------|-----------------|----------|----------|----------|
| | Case 1 U=0,V=0, H = 10. | | | | | | | |
| H km | ? | ? | ? | ? | | | | |
| U m/sec | 0.12 | 1.33 | 5.60 | 13.37 | | | | |
| V m/sec | 0.13 | 1.45 | 5.82 | 13.59 | | | | |
| | Case 2 U=10,V=0 | | | | Case 3 U=0,V=10 | | | |
| H km | ? | ? | ? | ? | ? | ? | ? | ? |
| U m/sec | 0.21 | 1.41 | 5.85 | 12.11 | 0.19 | 1.48 | 5.67 | 13.37 |
| V m/sec | 0.13 | 1.40 | 6.06 | 14.73 | 0.13 | 1.37 | 5.51 | 12.83 |

Table 3: Simulation errors of two satellites flying in formation, 1000 second difference in over flight. No height information is available.

Errors in the satellite ephemeris will lead to systematic errors when combining observations from two platforms. With careful inspection of the imagery, these errors can often be removed for areas with land marks. This was the case for the examples worked out below. Without improvement in the satellite navigation, application of this method to open ocean areas will often be subject to large systematic errors.

RESEARCH ACCOMPLISHED

Alaska case study

Figure 2 shows an image from POLDER of clouds over Alaska near Point Barrow (71°N, -156°W). The imaged area is roughly 1000x1000 km²; the continent being in the lower-right third as indicated by the coastline. The analysis proceeds by selecting a circular patch of pixels at the center time of the sequence, then searching for the maximum correlation in the other images in the sequence to estimate the location (**P**) of the cloud from the other times and view points (**S**). This matching was also performed with the remapped AVHRR image. The POLDER data has 6 km resolution visible pixels which would seem too large to provide stereo information, but in fact the correlation matching is able to measure the displacements to better than \pm one pixel. Aligning with the edge of an extended object provides enough information to estimate positions to about \pm 2 km (Campbell 1998). This set of apparent locations, viewpoints, and times were analyzed with the Asynchronous Stereo scheme (Campbell, 1998). This performs a least squares fit to estimate the height and motion of the object as was done in the simulation.

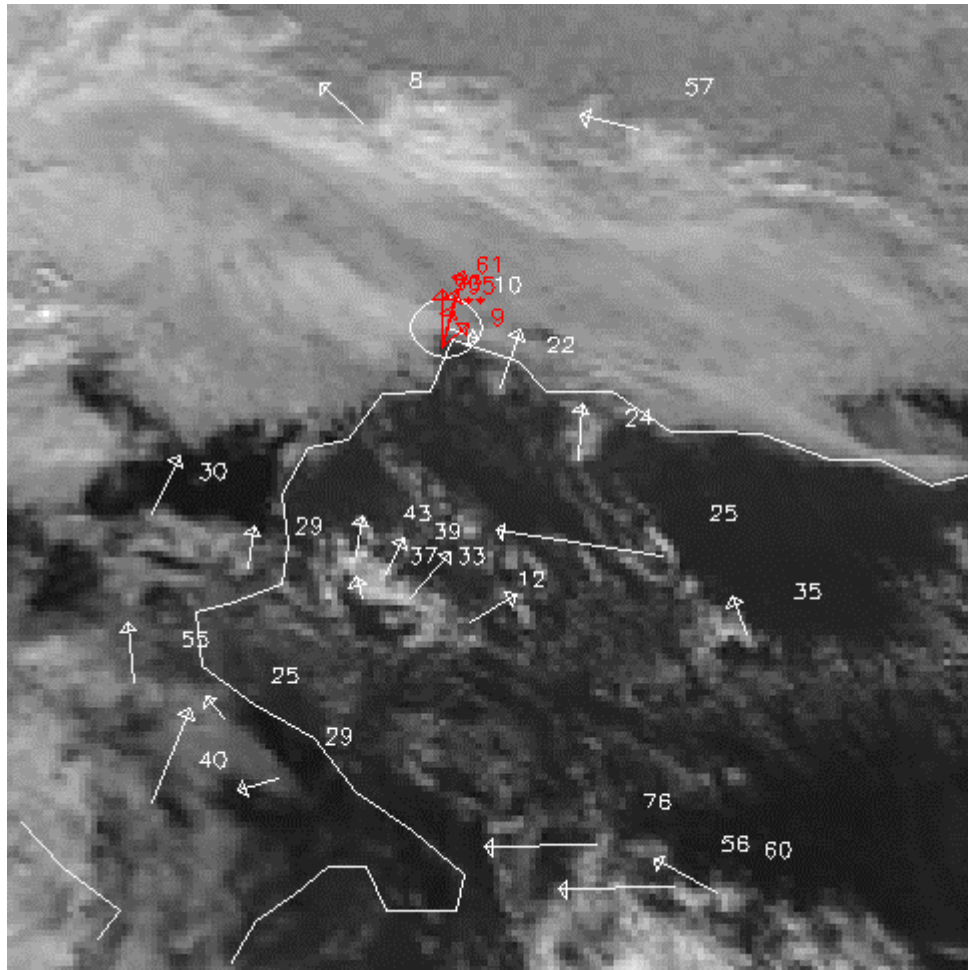


Figure 2: Image of Polder visible radiances over Alaska on June 19, 1997 at 22:30Z. Super imposed are estimates of the cloud motions and heights (hectometers). The wind rose in the circle shows the Point Barrow radiosonde at 0Z, June 20.

Shown in figure 2 are the cloud motion vectors and an estimate of the height. For instance the cloud over the land south of Point Barrow in the image is moving north at about 4km altitude. In the circle are the corresponding winds at different heights from the Point Barrow radiosonde. The wind at Point Barrow at 4 km height was 10.3 m/sec at 197° and the motion of the cloud was $7. \pm 2.$ m/sec, at $206^\circ \pm 13^\circ$. These not coincident in time, so a precise match should not be expected. Figure 3 shows the sounding with the water vapor profile showing a cloud top at 3.5 km (650 mb).

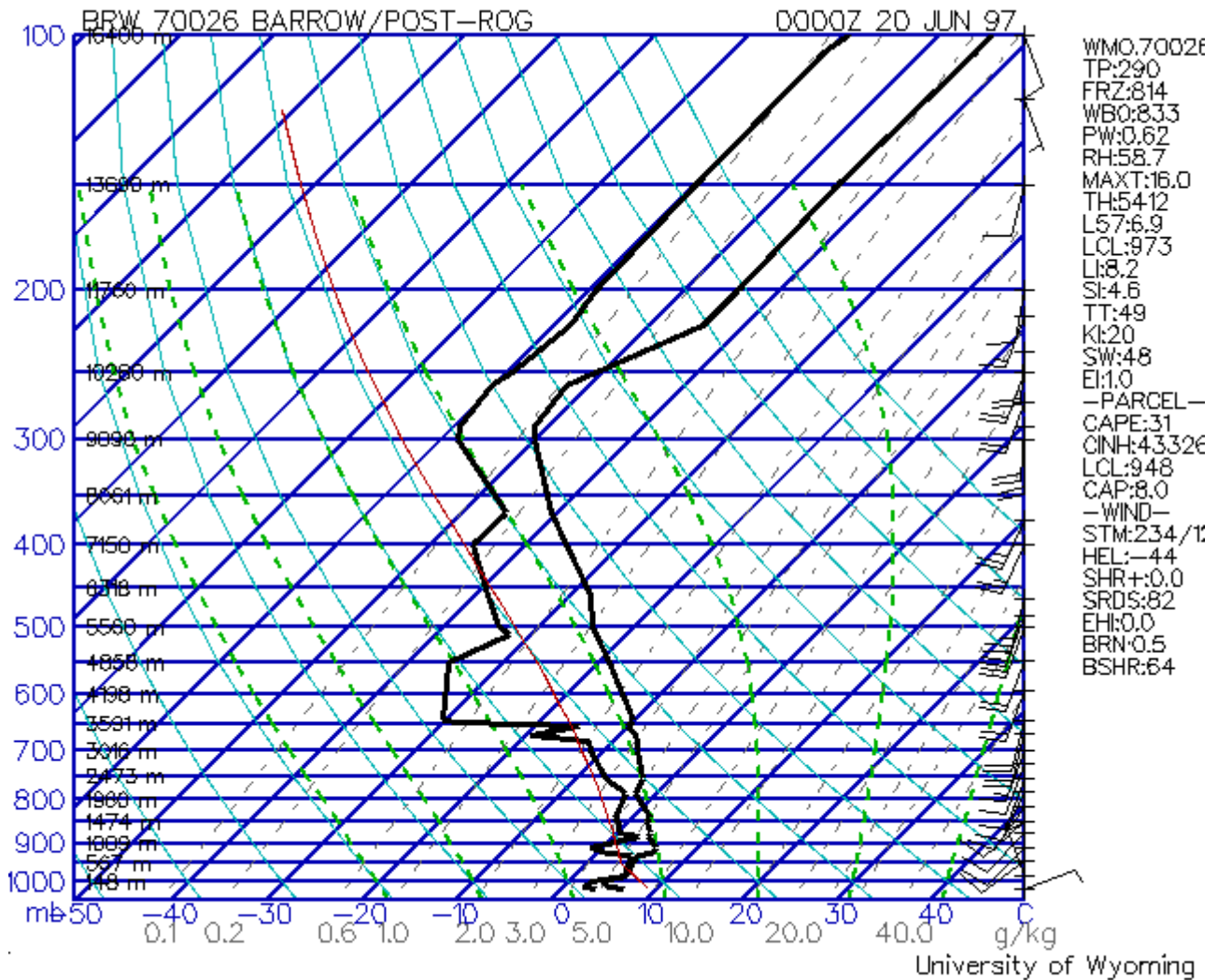


Figure 3. Point Barrow sounding

To get some empirical estimate of the accuracy of the measurements, some test clouds were tracked repeatedly, starting at locations offset \pm one pixel east-west and north-south. Table 4 shows a list of the heights, motions and standard deviations from this reproducibility study. This is really a test of the tracking procedure and small errors in matching the clouds from the different scenes. Table 3 is the source of the ± 2 km uncertainty in position matching for POLDER, which we suggested in the simulation discussion.

| Averages (5 trials) | | | Standard Deviations (5 trials) | | |
|---------------------|-----------|-----------|--------------------------------|-----------|-----------|
| Height | U (m/sec) | V (m/sec) | Height | U (m/sec) | V (m/sec) |
| 0.73 | -2.72 | 1.60 | 0.26 | 0.69 | 0.30 |
| -0.39 | 0.85 | 3.80 | 0.13 | 0.38 | 0.33 |
| 3.39 | 0.51 | 7.02 | 0.04 | 0.28 | 0.14 |
| 4.66 | 3.82 | 5.77 | 0.45 | 0.70 | 1.17 |

| | | | | | |
|------|-------|-------|------|------|------|
| 2.67 | -4.66 | 0.09 | 0.19 | 0.76 | 0.20 |
| 2.30 | 3.97 | 7.63 | 0.34 | 1.36 | 1.07 |
| 1.17 | 0.69 | -0.87 | 0.24 | 1.87 | 1.13 |
| 0.45 | 0.70 | 1.17 | 0.49 | 1.30 | 1.26 |

Table 4 Sample reproducibility test. Av = average of 5 heights, sd = standard deviation of the 5.

Baja case study

A second example was analyzed merging GOES and Polder viewing clouds over Baja, Mexico shown in figure 4. Here we were able to make a comparison with the geometric cloud analysis of GOES 8 plus GOES 9. This comparison of two geometric techniques is a better measure of the accuracy of the analysis. Figure 4 shows a systematic motion of the island in the Gulf of California. This is an indication of a misalignment in the navigation of GOES and POLDER. Errors in the satellite ephemeris will lead to systematic errors when combining observations from two platforms. With careful inspection of the imagery, these errors can often be removed for areas with land marks. This was the case for the examples worked out below. Without improvement in the satellite navigation, application of this method to open ocean areas will often be subject to large systematic errors.

In both these case studies, the navigation from the two satellites was misaligned. It was necessary to shift the imagery about 9 km in the Alaska case and 5 km in the Baja case discussed below. These systematic errors are a bigger problem than the noise from tracking the clouds. These adjustments are possible if land marks can be identified, but the adjustments would be more difficult over open ocean areas.

Figure 5 shows the POLDER plus GOES result with hand adjusted navigation to remove the motion of the island. Figure 6 shows the GOES analysis, which actually appears more consistent in the cloud motions and heights than the Polder result (fig 3). The GOES data was actually mapped into the Polder projection at 6 km resolution before the analysis.

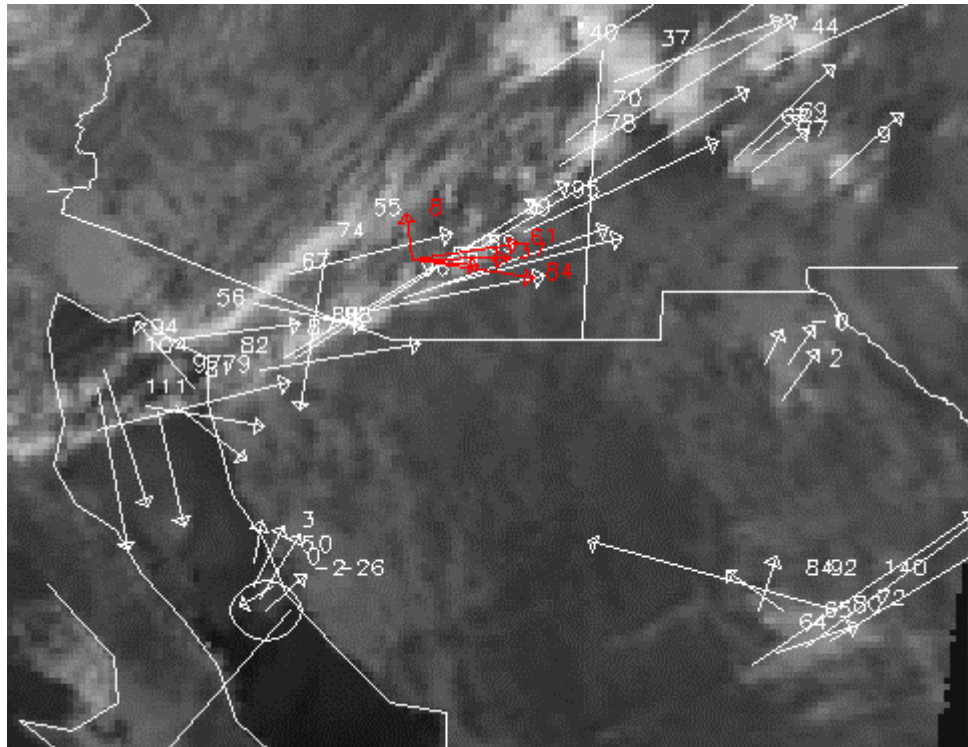


Figure 4: Polder visible radiances over Baja on April 29, 1997, 18:47Z. The heights are shown in hectometers. The navigation was adjusted to force no motion in the islands. The Tucson sounding winds are shown in red. Notice that the island have a systematic motion.

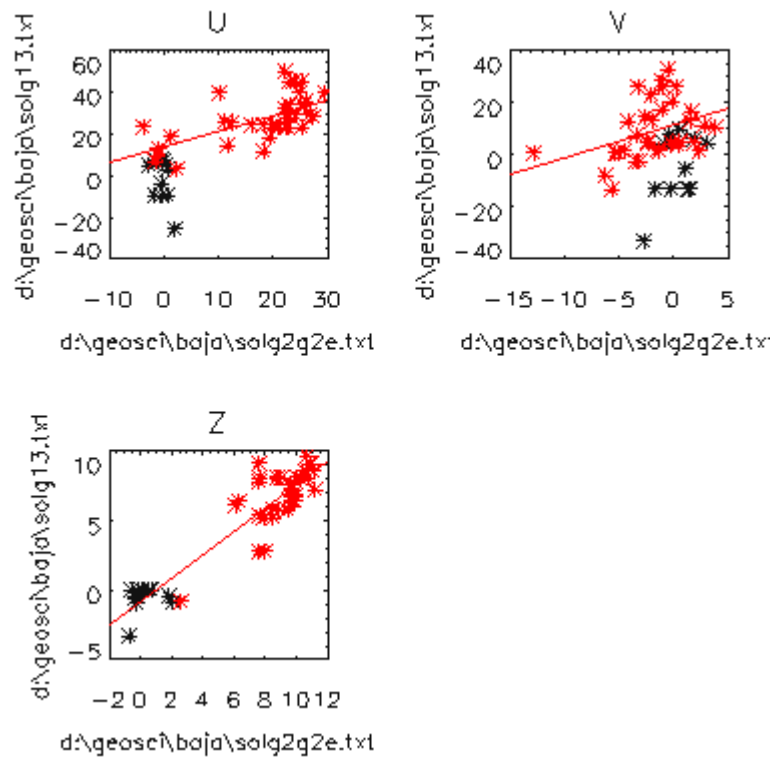


Figure 7: Scatter between GOES 8 and 9 results and Polder plus GOES 9 results. U and V are the components of the cloud motion and Z is the height (km). The GOES results are on the horizontal axes and the POLDER plus GOES on the vertical axes. The black symbols represent land features and the cloud are shown in red.

Figure 7 shows scatter diagrams of the heights of the two geometric analyses over Baja. The cloud were matched in location because the same set of starting locations was used for each analysis. From the scatter of the heights and the variation in cloud motion vectors in figure 3, there are many spurious wind vectors, which might be discarded with some spatial consistency check. (That is a standard procedure in operational wind analyses (Nieman et al, 1997)). Still the results of the POLDER analysis is not as consistent as the GOES analysis. Certainly, where available the GOES results would be more useful than the POLDER estimates.

The wind direction at 10 km matches well with the cloud motions estimated by both schemes as seen in figure 8. Interestingly there is no indication of the cirrus clouds in the sounding water vapor profile.

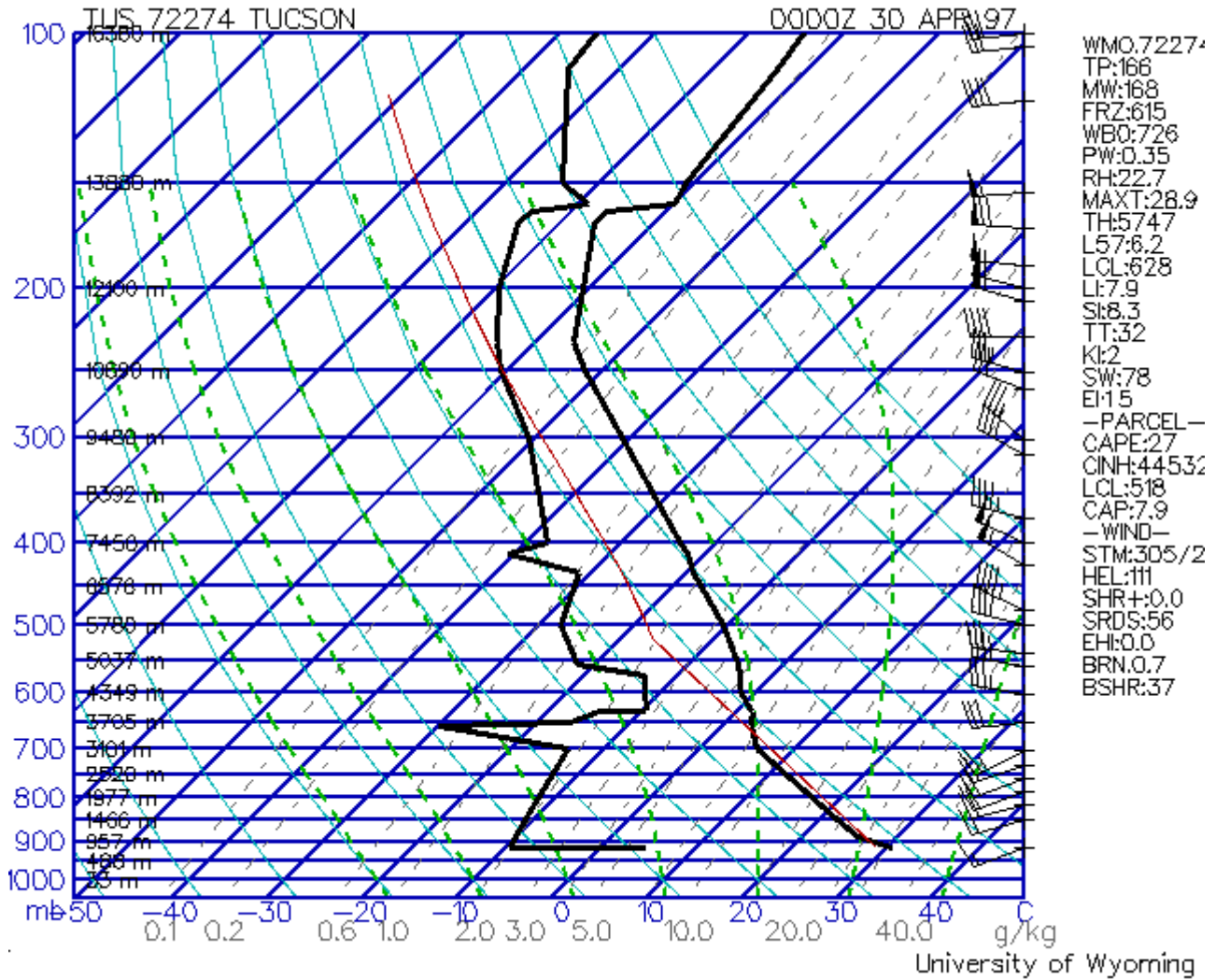


Figure 8 Tucson sounding showing motion wind at 10km in a direction matching the cloud motion, but there is no evidence of the cloud in the sounding.

Discussion

The goal of these analysis schemes is an automated global analysis of geometric height and cloud motion. Some of the spurious cloud motions in Figure 2 could be eliminated by spatial consistency checks. The simulation results suggest that the POLDER results are at the limit of signal exceeding the noise. A multiple-view instrument optimized to measure cloud motions and heights would require 1 km or better resolution.

Automating a scheme like this requires first remapping and aligning the images, second selecting candidate cloud edges, third tracking those edges, and fourth solving for the motion and heights. Finally the consistency check would filter vectors with large deviations. With the limited accuracy of POLDER results this work is not merited, unless some special experiment or case study needs cloud motion estimates where there is no other wind estimates.

With five operational geosynchronous weather satellites, cloud motions can be estimated with better accuracy in the tropics and mid latitudes. Geometric heights can be calculated with any combination of geosynchronous combination or geosynchronous plus polar combination, not just a multiple view instrument. The special utility of multiple view stereo is then limited to the polar regions. With a better resolution instrument like MISR, consideration should be given to geometric analysis of clouds. Data from MISR should be available in the spring of 2000 and some experiments like these will be performed for polar areas.

Oxygen A band heights

In addition to the bi-directional imaging capabilities of POLDER, there are two channels which measure the reflected radiance in the Oxygen A absorption band at 765 nm. The ratio of the two observed radiances provide a measure of the oxygen absorption between the satellite and the reflection surface, assumed to be a spectrally white reflector. Because the oxygen is well mixed in the atmosphere, this absorption is related to the height of the cloud (Parol et al. 1999). Figure 9 shows an image of the cloud top pressure estimate based on this differential absorption technique.

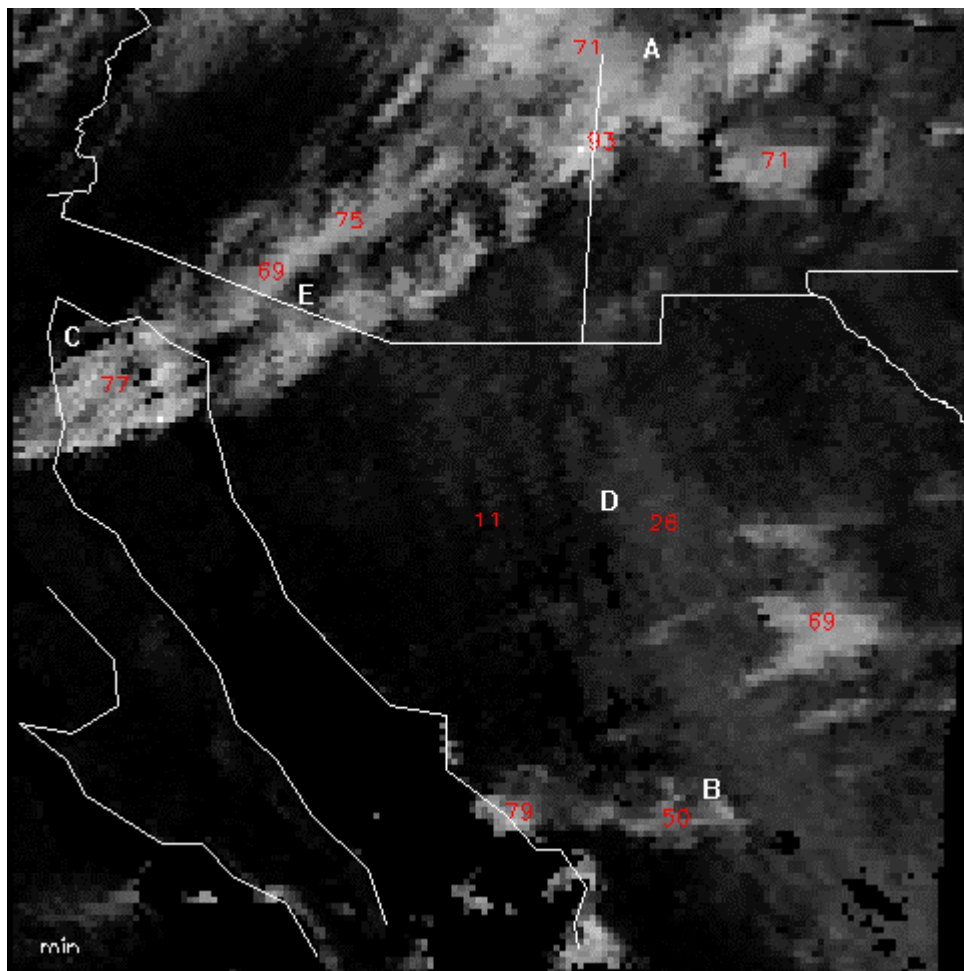


Figure 9 Image of Oxygen A band heights. The numbers are heights in hectometers derived from the Tucson sounding. The minimum height from the 14 views of each location.

This shows some artifacts. The cirrus clouds over the Gulf of California are higher than those adjacent over the land. There is considerable variability from one view point to the next for the same cloud. It turns out that the cloud is not a simple reflecting surface. Some of the visible radiation is scattered within the cloud top and some of the radiation from ground penetrates the cloud (Parol et al. 1999). These contaminate the Oxygen absorption signals. Figure 9 is actually a composite of the minimum cloud height over the 14 views of the cloud masking some of the variability of the estimates.

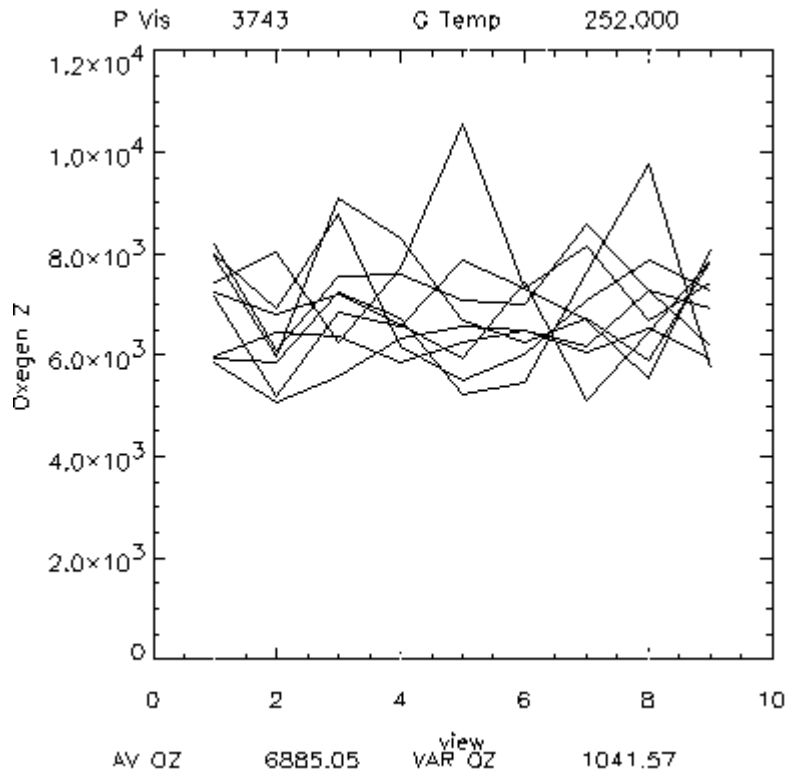


Figure 10: Heights of adjacent pixel from 10 views of a cloud over the ocean area.

Using the Tucson sounding, the pressures were converted to geometric height for comparison to the Asynchronous heights. Finally figure 6 shows a scatter plot of the geometric heights and the Oxygen heights. The Oxygen heights show considerable variability in space and from the many view points so these are the lowest heights in the region from the multiple view points.

The standard way to estimate cloud top height is to use the cloud top temperature and a temperature profile estimate. For comparison the cloud heights in table 5 were estimated by interpolation from the Tucson sounding. Similarly, Figure 11 shows a scatter plot of the two height estimations: geometric and Oxygen absorption. Clouds are certainly separated from surface, but scatter shows that neither method is precise.

| Table 2 | Oxygen Z (km) | Geometric Z | GOES Temperature | Temperature > Z |
|----------------|---------------|-------------|------------------|-----------------|
| A | 5.6 | 4.7 | 234 | 9.3 |
| B Cirrus ocean | 8.6 | 8.6 | 242 | 8.2 |
| C | 8.0 | 6.8 | 243 | 8.1 |
| D | 8.5 | 6.9 | 228 | 10. |
| E | 3.7 | 7.3 | 233 | 10. |
| F | 7.4 | 5.1 | 242 | 8.2 |
| G | 7.0 | 6.8 | 243 | 8.1 |

Table 5: Selected points from figure 9 analyzed several ways. Heights in km and temperature in Kelvin.

The Oxygen A band heights show some skill but there are some artifacts with different backgrounds and cloud types. Using the geometric cloud height estimates could be used as a verification tool to better understand the variability of the Oxygen method and filter out the unphysical height estimates. These anomalous heights are an indication of other physical processes are occurring in the reflections from the cloud like multiple scattering in the cloud or transmission of light from the underlying surface.

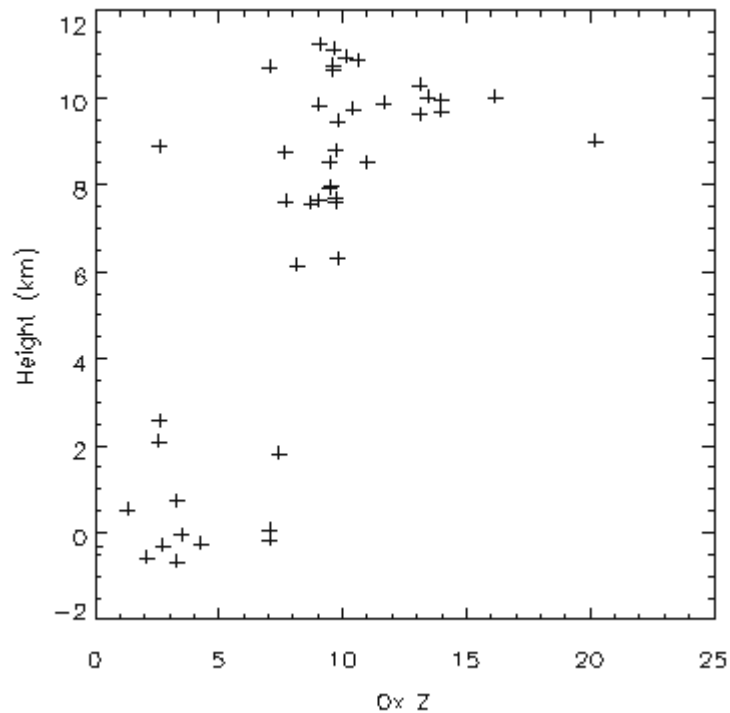


Figure 11 Comparison of geometric heights with Oxygen heights, Baja case. Geometric height on the vertical axis and Oxygen A band cloud top pressures converted to height with a nearby sounding.

CONCLUSIONS AND RECOMMENDATIONS

The geometric analysis of cloud motion and height is possible with polar observations. The POLDER instrument resolution is just barely able to make measurements beyond the noise, so an extensive effort to automate the analysis is not warranted. The analysis of Oxygen A band absorption must be more sophisticated. It will require many bands, not just a narrow and broad band to understand the cloud properties as well as the height. Tests should be performed with MISR data from Terra where very accurate results should be possible with the inclusion of another satellite. Also pairs of DMSP satellite following each other in the same orbit may offer the possibility of measuring cloud motion from the 15 to 30 minute separation of the over flights, but not geometric heights.

Animations will be provided on the CD distributed from the meeting. [Click here for animations.](#)

Acknowledgements

This work was supported by the Department of Defense Center for Geosciences/Atmospheric Research Agreement #DAAL01-98-2-0078. The results presented in this paper were obtained using data from CNES/POLDER onboard NASDA/ADEOS. Some of this research was reported at the World Meteorological Fifth Winds Workshop, 2000 (Campbell and Breon, 2000)

References

Campbell, G.G., 1998, Asynchronous Stereo Height and Motion Analysis: Applications, Fourth Winds Workshop, WMO.

Campbell, G.G. and F.-M. Breon, 2000, Polar Orbiter: Stereo Heights and Cloud Motions, Fifth WMO Winds Workshop, Melbourne, Australia

Deschamps, O.Y., F.M. Breon, M. Leroy, A. Opodaire, A. Bricaud, J.C. Buriez, and G. Seze; 1994, The POLDER mission: Instrument characteristics and scientific objectives., *IEEE Trans. Geosci. Remote Sensing*, vol 32, PP 598-614.

Menzel, P., 2000, Cloud tracking with satellite imagery: From the pioneering work of Ted Fujita to the present, *BAMS*, accepted.

Nieman, S. 1997, Fully automated cloud-drift winds in NESDIS operations, *Bull. Amer. Meteor. Soc.*, **78**, 1121-1134.

Parol, F., J-C Buriez, C. Vanbauce, P. Couvert, G. Seze, P. Goloub, and S. Cheinet, 1999, First results of POLDER "Earth radiation budget and clouds" operational algorithm, *Trans. On Geoscience and Remote Sensing*, Vol 37, No. 3, 1597-1612.